9-27-2004

Speckle Reduction of SAR Images Based on a Combined Markov Random Field and Statistical Optics Approach (Version1)

Ousseini Lankoande

Majeed M. Hayat

Bal Santhanam

DEPARTMENT OF ELECTRICAL AND COMPUTER ENGINEERING

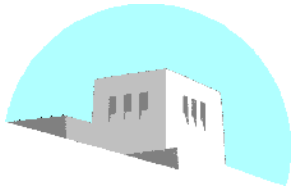

SCHOOL OF ENGINEERING

UNIVERSITY OF NEW MEXICO

Speckle Reduction of SAR Images Based on a Combined Markov Random Field and Statistical Optics Approach (Version1)

Ousseini Lankoande
Department of Electrical and Computer Engineering
The University of New Mexico
Albuquerque, NM 87131
e-mail: lankoande@ece.unm.edu

Majeed M. Hayat
Department of Electrical and Computer Engineering
The University of New Mexico Albuquerque, NM 87131
Phone: (505) 277-0297, Fax: (505) 277-1439
e-mail: hayat@ece.unm.edu

Balu Santhanam
Department of Electrical and Computer Engineering
The University of New Mexico Albuquerque, NM 87131
Phone: (505) 277-1611, Fax: (505) 277-1439
e-mail: bsanthan@ece.unm.edu

UNM Technical Report: EECE-TR-2004-21

Report Date: September 27, 2004

Abstract

One of the major factors plaguing the performance of synthetic aperture radar (SAR) imagery is the signal-dependent, speckle noise. Grainy in appearance, it is due to the phase fluctuations of the electromagnetic returned signals. Since the inherent spatial-correlation characteristics of speckle in SAR images are not embedded in the multiplicative models for speckle noise, a new approach is proposed here that provides a new mathematical framework for modeling and mitigation of speckle noise. The contribution of this report is thus twofold. First, a novel model for speckled SAR imaging is introduced based on Markov random fields (MRFs) in conjunction with statistical optics. Second, utilizing the model, a global energy-minimization algorithm, the simulated annealing (SA), is introduced for speckle reduction. In particular, the joint conditional probability density function (cpdf) of the intensity of any two points in the speckled image and the associated correlation function are used to derive the cpdf of the center pixel intensity given its four neighbors. The Hammersley-Clifford theorem is then used to derive the energy function associated with the MRF. The SA built on the Metropolis sampler, is employed for speckle reduction. Four metrics are used to assess the quality of the speckle reduction: the mean-square error, SNR, an edge-preservation parameter and the equivalent number of looks. A comparative study using both simulations and real SAR images indicates that the proposed approach performs well compared to filtering techniques such as the Gamma Map, the modified Lee and the enhanced Frost algorithms.

Keywords

speckle modeling, speckle reduction, synthetic aperture radar, SAR imaging, Markov random fields.

1 Introduction

Synthetic aperture radar (SAR) is a type of imaging system that uses coherent radiation to create images. The major advantage of SAR over non-radar imaging systems is that it does not rely on an external source. As an active system, SAR emits its own radiations and remains effective independently of weather or daylight conditions [9]. Unfortunately, this autonomy comes with a higher susceptibility to speckle noise.

A SAR system coherently records the amplitude and the phase echoed from a target. Since each resolution cell of the system contains several scatterers, and since the phases of the returned signals from these scatterers are randomly distributed, the inherent coherent processing involved results in interference noise like patterns also called speckle. A large variety of speckle-reduction techniques have been proposed in the literature. Among them are the Lee filter and its derivative [13, 15], the geometric filter [4], the Kuan filter [12], the Frost filter and its derivative [15, 11], the Gamma MAP filter [15], the wavelet approach [2, 7] and the *Markov-random-field* (MRF) approach [17, 8]. In this report, we will focus on two issues: the modeling of speckled imagery and speckle reduction. What is unique about our MRF model is that it is based on the physics of the speckle phenomenon. In particular, we merge the concept of a MRF with statistical properties of speckle from optics and use this model to implement speckle reduction using simulated annealing (SA).

2 First order MRF model

A MRF consists of an undirected graph $G = (V,E)$, which has undirected edges drawn as lines. The set V of vertices of the graph is $\{I_k, I_{k_1}, I_{k_2}, I_{k_3}, I_{k_4}\}$ and E is the set of edges. Two type of cliques can be defined for the graph in Figure 1. The single-clique, $C_1 = \Big\{(x_k,y_k), k \in S\Big\}$, and the pair-clique, $C_2 = \Big\{ \{(x_k,y_k),(x_{k_1},y_{k_1})\},\{(x_k,y_k),(x_{k_2},y_{k_2})\},\{(x_k,y_k),(x_{k_3},y_{k_3})\},\{(x_k,y_k),(x_{k_4},y_{k_4})\}\ k \in S, k_i \in S, i = 1,\cdots,4 \Big\}$, where S is the set of indexes of the image.

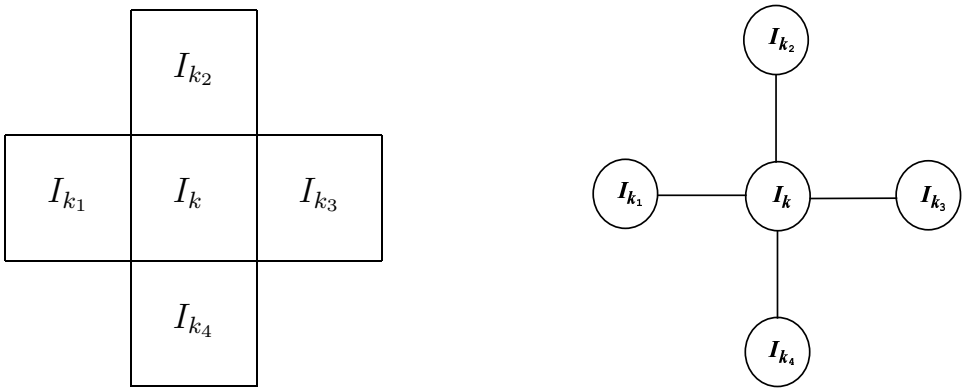

(a) **(b)**

Figure 1: (a) First order neighborhood (lattice form). (b) Graph of the first order neighborhood.

2.1 Conditional probability density specification

The *conditional probability density* (cpd) function of the intensity I_{k_j} at point k_j given the value of the intensity I_{k_i} at point k_i is given by Goodman in [5]. Here, the global mean, $\langle I \rangle$, has been substituted by $(i_t)_{k_j}$, which is

defined as the true intensity image at point k_j. The realization of the random variable I_{k_j} at point k_j is denoted by i_{k_j}. More precisely,

$$p_{I_{k_j}|I_{k_i}}(i_{k_j}|i_{k_i}) = \frac{e^{-\frac{|\mu(r_{k_ik_j})|^2 i_{k_i}+i_{k_j}}{(i_t)_{k_j}(1-|\mu(r_{k_ik_j})|^2)}}}{(i_t)_{k_j}(1-|\mu(r_{k_ik_j})|^2)} \times I_0\Big(\frac{2\sqrt{i_{k_i}i_{k_j}}|\mu(r_{k_ik_j})|}{(i_t)_{k_j}(1-|\mu(r_{k_ik_j})|^2)}\Big), \tag{1}$$

where $I_0(\cdot)$ is a modified Bessel function of the first kind and zero order, and $|\mu(r_{k_ik_j})|$ and $r_{k_ik_j}$ are, respectively, the coherence factor and the Euclidian distance between the points k_i and k_j. We define the coherence factor as follows:

$$|\mu(r_{k_ik_j})| = \begin{cases} |\alpha_{r_{k_ik_j}}| \in [0,1[& \forall\, r_{k_ik_j} \le 1 \\ 0 & \text{otherwise.} \end{cases} \tag{2}$$

Note that if $r_{k_ik_j} > 1$ then (1) becomes independent of i_{k_i} and equal to $p_{I_{k_j}}(i_{k_j}) = e^{-\frac{i_{k_j}}{(i_t)_{k_j}}}/(i_t)_{k_j}$. In addition, in (2) the correlation is assumed to be limited to one unit from the center pixel. This condition can still be met with larger correlation (more than one unit correlation) by preprocessing the data. Indeed, in the case of an image having a larger correlation we will apply one of the interpolation methods in order for the correlation to fit the above definition of the coherence factor [8]. The Euclidian distance between the pair of pixels (i_{k_1}, i_{k_2}), (i_{k_2}, i_{k_3}), (i_{k_3}, i_{k_4}), (i_{k_4}, i_{k_1}),(i_{k_2}, i_{k_4}) and (i_{k_1}, i_{k_3}), is either $\sqrt{2}$ or 2; in both cases, the distance is greater than 1 unit. Using the coherence factor defined in (2), we can conclude that these pairs of pixels are conditionally independent given the center pixel i_k. Then cpd function of the intensity of the center pixel, i_k, given the four neighbors i_{k_1}, i_{k_2}, i_{k_3} and i_{k_4} takes the following form

$$p_{I_k|I_{k_1},I_{k_2},I_{k_3},I_{k_4}}(i_k|i_{k_1},i_{k_2},i_{k_3},i_{k_4}) = \frac{p_{I_k|I_{k_1}}(i_k|i_{k_1})p_{I_k|I_{k_1}}(i_k|i_{k_1})p_{I_k|I_{k_1}}(i_k|i_{k_1})p_{I_k|I_{k_1}}(i_k|i_{k_1})}{\Big(p_{I_k}(i_k)\Big)^3} \tag{3}$$

Recall that each term in (3) is precisely known using (1). Therefore, after substitution we obtain

$$\begin{aligned} p_{I_k|I_{k_1},I_{k_2},I_{k_3},I_{k_4}}(i_k|i_{k_1},i_{k_2},i_{k_3},i_{k_4}) &= \frac{e^{-\sum_{j=1}^4 \frac{A(i_k,i_{k_j})}{B(i_k,i_{k_j})}} \prod_{j=1}^4 I_0(\frac{C(i_k,i_{k_j})}{B(i_k,i_{k_j})})}{(p_{I_k}(i_k))^3 \prod_{j=1}^4 B(i_k,i_{k_j})} \\ &= \frac{e^{-\sum_{j=1}^4 \frac{A(i_k,i_{k_j})}{B(i_k,i_{k_j})}} e^{\sum_{j=1}^4 \ln(I_0(\frac{C(i_k,i_{k_j})}{B(i_k,i_{k_j})}))}}{e^{\ln(p_{I_k}(i_k))^3)} e^{\sum_{j=1}^4 \ln(B(i_k,i_{k_j}))}} \\ &= e^{-\sum_{j=1}^4 \frac{A(i_k,i_{k_j})}{B(i_k,i_{k_j})}} e^{\sum_{j=1}^4 \ln(I_0(\frac{C(i_k,i_{k_j})}{B(i_k,i_{k_j})}))} e^{-\sum_{j=1}^4 \ln(B(i_k,i_{k_j}))} e^{-3\ln(p_{I_k}(i_k))} \\ &= e^{-\sum_{j=1}^4 \frac{A(i_k,i_{k_j})}{B(i_k,i_{k_j})} + \sum_{j=1}^4 \ln(I_0(\frac{C(i_k,i_{k_j})}{B(i_k,i_{k_j})})) - \sum_{j=1}^4 \ln(B(i_k,I_{k_j})) - 3\ln(p_{I_k}(i_k))} \end{aligned}$$

And finally,

$$p_{I_k|I_{k_1},I_{k_2},I_{k_3},I_{k_4}}(i_k|i_{k_1},i_{k_2},i_{k_3},i_{k_4}) = e^{-\sum_{j=1}^4 \ln(B(i_k,i_{k_j})) - \sum_{j=1}^4 \frac{A(i_k,i_{k_j})}{B(i_k,i_{k_j})} + \sum_{j=1}^4 \ln(I_0(\frac{C(i_k,i_{k_j})}{B(i_k,i_{k_j})})) - 3\ln(p_{I_k}(i_k))} \tag{4}$$

where $A(i_k,i_{k_j}) = |\alpha_{r_{kk_j}}|^2 i_{k_j} + i_k$, $B(i_k,i_{k_j}) = (i_t)_k(1-|\alpha_{r_{kk_j}}|^2)$, and $C(i_k,i_{k_j}) = 2\sqrt{i_k i_{k_j}}|\alpha_{r_{kk_j}}|$.

2.2 Energy and potential function

We observe that the cpd function obtained in (4) has the form

$$p_{I_k|I_{k_1},I_{k_2},I_{k_3},I_{k_4}}(i_k|i_{k_1},i_{k_2},i_{k_3},i_{k_4}) = e^{-U(i_k,i_{k_1},i_{k_2},i_{k_3},i_{k_4})} \tag{5}$$

where,

$$U(i_k,i_{k_1},i_{k_2},i_{k_3},i_{k_4}) = V_{C_1}(i_k) + V_{C_2}(i_k,i_{k_1},i_{k_2},i_{k_3},i_{k_4}), \tag{6}$$

$$V_{C_1}(i_k) = 3\ln(p_{I_k}(i_k)),$$

$$V_{C_2}(i_k,i_{k_1},i_{k_2},i_{k_3},i_{k_4}) = \sum_{j=1}^{4}\Big(\frac{A(i_k,i_{k_j})}{B(i_k,i_{k_j})} - \ln\Big(I_0\big(\frac{C(i_k,i_{k_j})}{B(i_k,i_{k_j})}\big)\Big) + \ln\big(B(i_k,i_{k_j})\big)\Big).$$

From the Hammersley-Clifford theorem [3], the energy function is identified to be $U(i_k,i_{k_1},i_{k_2},i_{k_3},i_{k_4})$. The terms $V_{C_1}(i_k)$ and $V_{C_2}(i_k,i_{k_1},i_{k_2},i_{k_3},i_{k_4})$ are, respectively, the single-clique and the pair-clique potential functions.

3 Simulation and Experimental Results

3.1 Image quality assessment parameters

The assessment of the speckle reduction quality will be based on four metrics. The first metric is the *mean square error* (MSE) between the noise-free and the denoised images having each K pixels; it is defined as follows

$$MSE = K^{-1}\sum_{i=1}^{K}(I_i - \widehat{I}_i)^2.$$

The second metric is the so-called β parameter used in [7], which assesses the quality of the edge preservation. It is defined by

$$\beta = \frac{\Gamma(\mathrm{I_H} - \overline{\mathrm{I_H}}, \widehat{\mathrm{I_H}} - \overline{\widehat{\mathrm{I_H}}})}{\sqrt{\Gamma(\mathrm{I_H} - \overline{\mathrm{I_H}}, \mathrm{I_H} - \overline{\mathrm{I_H}})\Gamma(\widehat{\mathrm{I_H}} - \overline{\widehat{\mathrm{I_H}}}, \widehat{\mathrm{I_H}} - \overline{\widehat{\mathrm{I_H}}})}}.$$

with $\Gamma(I_1,I_2) = \sum_{i=1}^{K} I_{1_i} I_{2_i}$. The best preservation coefficient is 1. The quantities I_H and $\widehat{I_H}$ are the highpass filtered versions of I and $\widehat{I}$, respectively (using the Laplacian operator), and I and $\widehat{I}$ represent the original (or noise free) and the noisy (or despeckle) intensity image, respectively. The third metric, which is the *signal-to-noise ratio* (SNR) in db is defined by

$$\mathrm{SNR} = 10\log_{10}\Big(\sum_{\mathrm{j}=1}^{\mathrm{K}} \mathrm{I_i}^2 \Big/ \sum_{\mathrm{j}=1}^{\mathrm{K}} (\mathrm{I_i} - \widehat{\mathrm{I}}_\mathrm{i})^2\Big).$$

The forth and final metric is the *effective number of looks* (ENL); it is often used to estimate the speckle noise level in a SAR image [8]. The higher the parameter the lower the speckle noise in the area will be. The ENL is used to assess the reduction performance not only on simulated but also on real speckled images. It is obtained by using the mean and variance intensity over a uniform area as follows

$$\mathrm{ENL} = \frac{(\mathrm{mean}^2)_{\mathrm{UniformArea}}}{(\mathrm{variance})_{\mathrm{UniformArea}}}$$

3.2 Simulated Annealing using the Metropolis sampler algorithm

In this section we describe the combined SA and *Metropolis sampler* (MS) scheme used for speckle reduction. The SA is a global energy-minimization algorithm [10]. It is applied on the MS at a gradually decreasing temperature T. Note that ΔU represents the energy difference between the candidate and the current configuration energy. This is where the energy obtained in (6) comes into play. The description of the SA-MS algorithm is summarized as follows:

Initialization Enter the image to process then set the initial temperature T_0 and the coherence factor $\alpha_{r_{kk_j}}$.

Step 1 : Start the SA process: Consider the k^{th} pixel with intensity i_k. Generate $i_{k_{\text{new}}} \in L \backslash \{i_{k_{\text{new}}}\}$ at random with $L \backslash \{i_{k_{\text{new}}}\}$ being the set of grey levels except $i_{k_{\text{new}}}$.

Step 2 : Update the temperature with $T_k = \lambda \times T_{k-1}$, where λ is a fixed parameter (here, λ is chosen as 0.97).

Step 3 : Compute $p = \min\{1, e^{-\Delta U / T_k}\}$, where $\Delta U = U(i_{k_{\text{new}}}, i_{k_2}, i_{k_3}, i_{k_4}) - U(i_k, i_{k_2}, i_{k_3}, i_{k_4})$.

Step 4 : Acceptance/Rejection step.

Generate a uniformly-distributed r.v. $R \in [0,1]$.

If $R < p$ then accept $i_{k_{\text{new}}}$, i.e., $i_k \leftarrow i_{k_{\text{new}}}$.

If $R \geq p$ then reject $i_{k_{\text{new}}}$, i.e., i_k is unchanged.

Step 5 : Increment k and go to Step-1 until $k = M \times N$, the $M \times N$ being the size of the image.

Steps 1-5 constitute one iteration of the SA scheme. The SA will be run until the equilibrium is reached then the despeckled image is returned.

3.3 Simulation of speckled images

In order to create a speckled image from an original image we feed the SA-MS algorithm with the original image and set the temperature to a fix value; here we have chosen $T_0 = 10$ (the results of other choices are presented later). The algorithm is run one time. The noise free images used in this work, are the aerial photographs of two scenes; they will be called photo1 and photo2, respectively [1]. Figures 2 and 3 show the result of the simulations. The SNR is used to calculate the information content. We will study now certain special cases: for a temperature T approaching zero, the Metropolis algorithm predicts no major change of the output compared to the current input; this is shown in Figure 4a and Figure 4b below. As the temperature T increases, so does the noise. This is shown in the Figures 5-8.

(a) **(b)**

Figure 2: (a) Original photo1. (b) Speckled version of photo1 with SNR=14.11 db.

(a) **(b)**

Figure 3: (a) Original photo2. (b) Speckled version of photo2 with SNR=14.34 db.

(a) **(b)**

Figure 4: (a) Speckled version of photo1 with $T_0 \rightarrow 0$ and SNR=25.66 db. (b) Speckled version of photo2 with $T_0 \rightarrow 0$ and SNR=27.84 db.

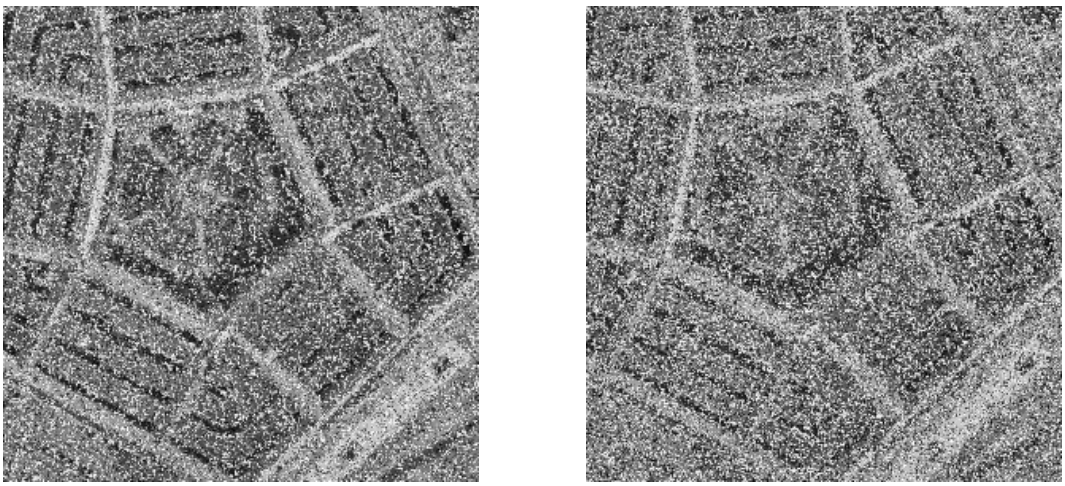

(a) **(b)**

Figure 5: (a) Speckled version of photo1 with $T_0 = 20$ and SNR=11.29 db. (b) Speckled version of photo1 with $T_0 = 30$ and SNR=10.27 db.

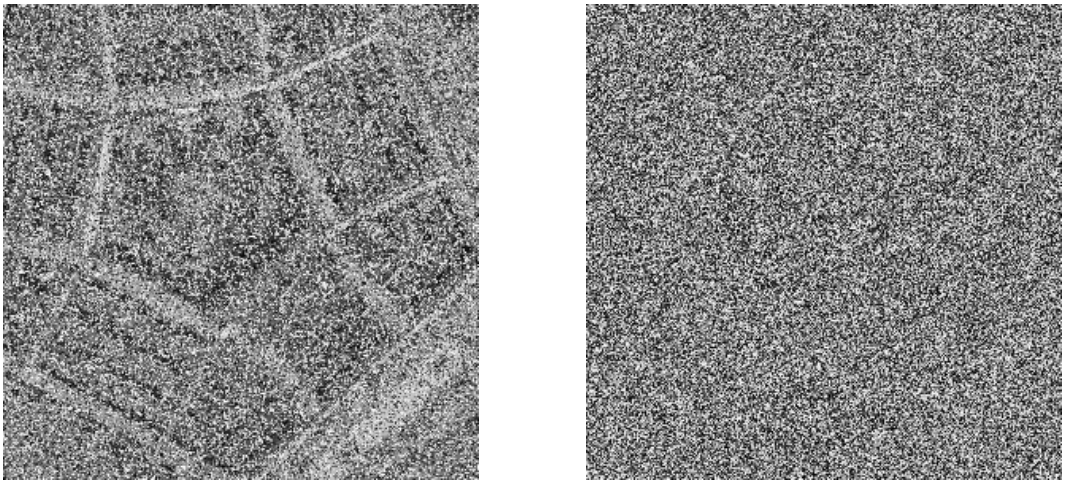

(a) **(b)**

Figure 6: (a) Speckled version of photo1 with $T_0 = 40$ and SNR=9.74 db. (b) Speckled version of photo1 with $T_0 = 500$ and SNR=7.74 db.

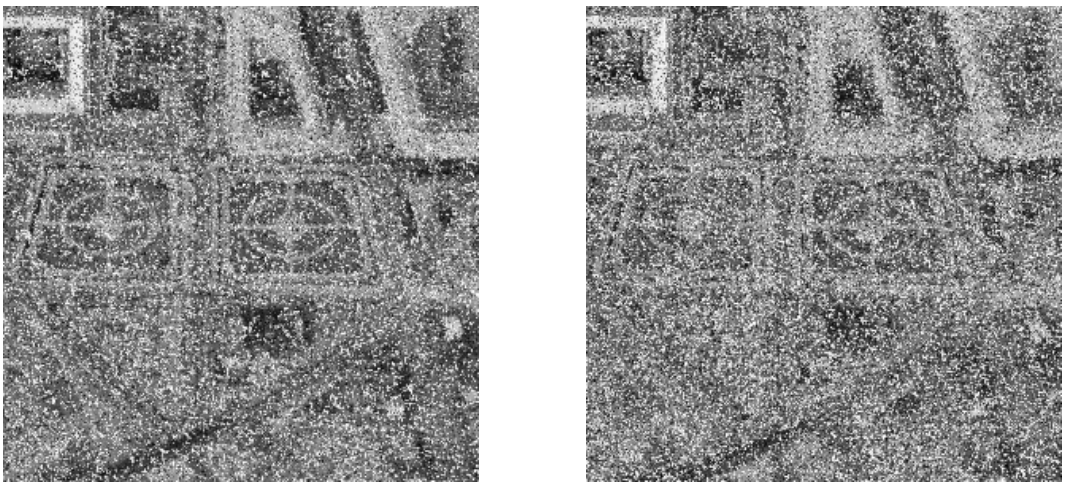

(a) **(b)**

Figure 7: (a) Speckled version of photo2 with $T_0 = 20$ and SNR=11.12 db. (b) Speckled version of photo2 with $T_0 = 30$ and SNR=9.92 db.

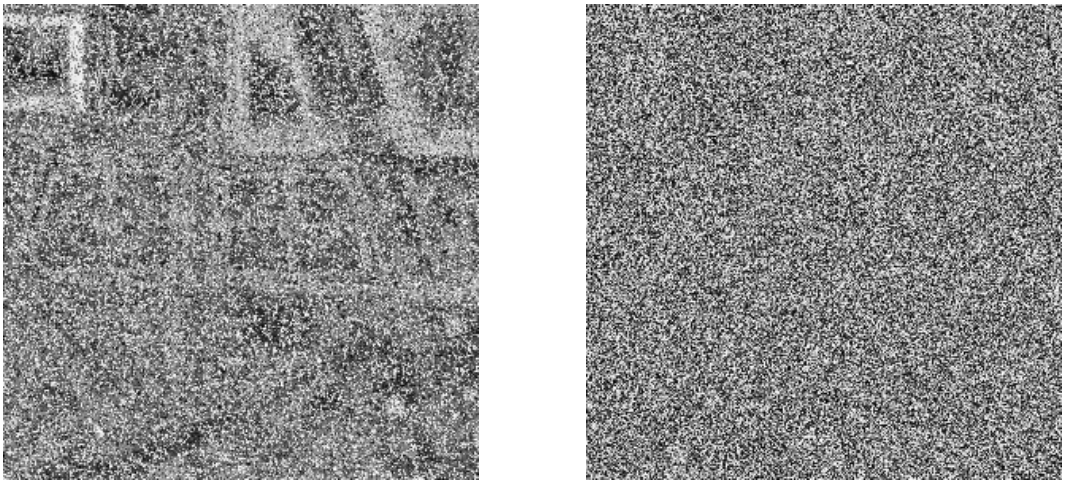

(a) **(b)**

Figure 8: (a) Speckled version of photo2 with $T_0 = 40$ and SNR=9.27 db. (b) Speckled version of photo2 with $T_0 = 500$ and SNR=7.06 db.

3.4 Speckle reduction of simulated speckled images

The goal here is to reduce the speckle existing in Figures 2b and 3b. We compare our proposed approach against well-known speckle removal filters: the Gamma Map, the modified Lee and the enhanced Frost filters [14, 15]. The results of the speckle reduction are presented in Figures 9-13 for photo1 on one hand and Figures 14-17 for photo2 on the other hand.

(a) **(b)**

Figure 9: (a) Original photo1. (b) Speckled version of photo1 with $T_0 = 10$ and SNR=14.11 db.

Tables I and II give a summary of the results. The metrics ENL, MSE, β, and SNR defined in section 3.1 are evaluated for the proposed approach and compared to the other filters. For both images tested (photo1 and

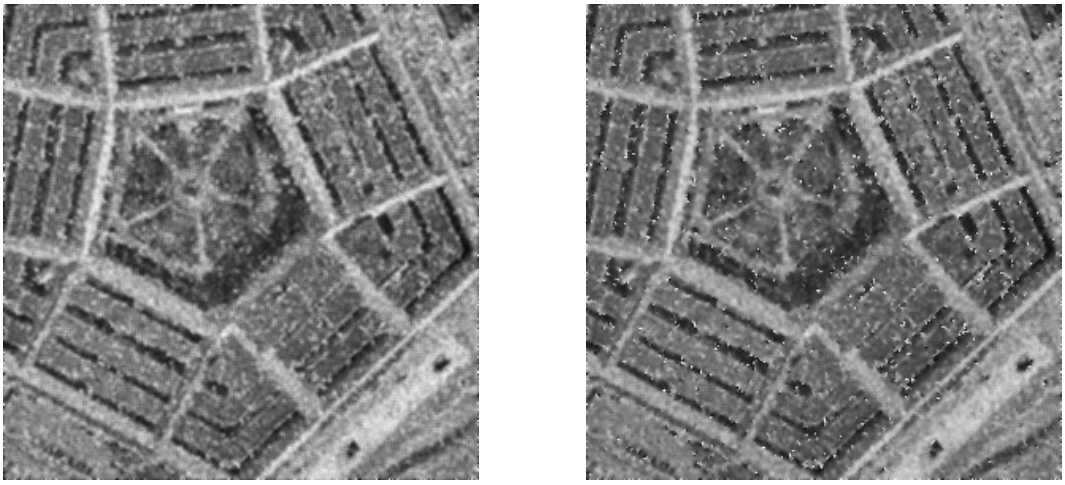

(a) **(b)**

Figure 10: (a) Modified-Lee filtered version. (b) Gamma filtered version.

photo2), around 40 iterations, our proposed approach outperforms the other filters based on all above four metrics.

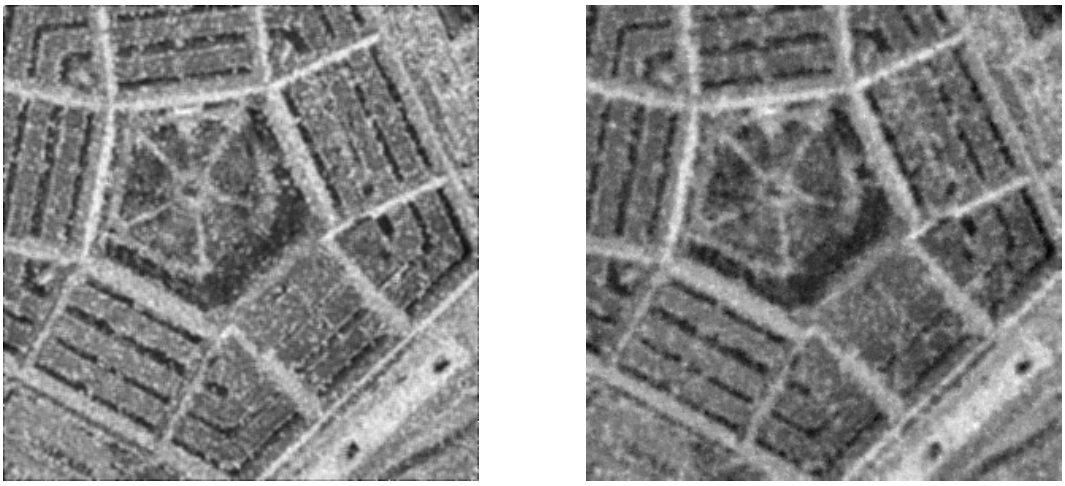

(a) **(b)**

Figure 11: (a) Frost Enhanced filtered version. (b) Proposed approach after 40 iterations.

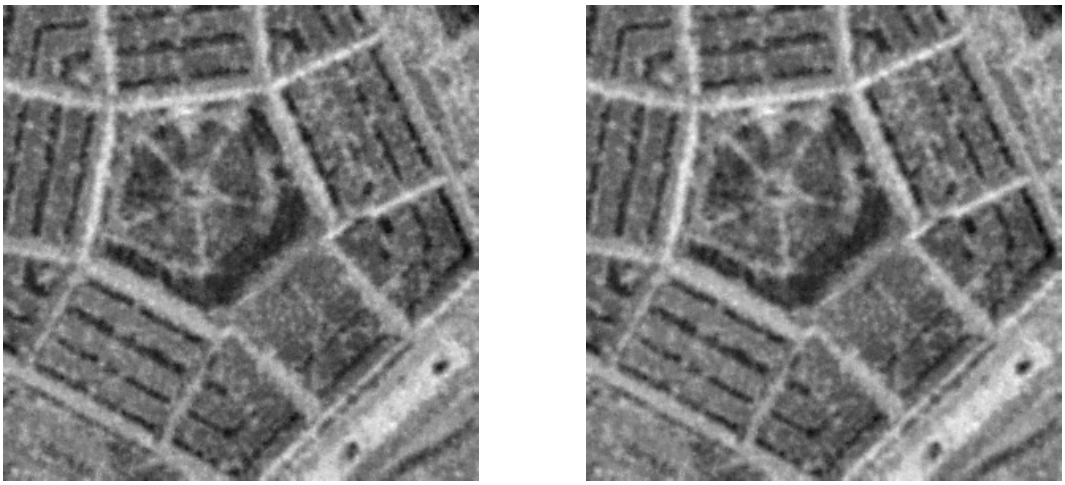

(a) **(b)**

Figure 12: (a) Proposed approach after 50 iterations. (b) Proposed approach after 60 iterations.

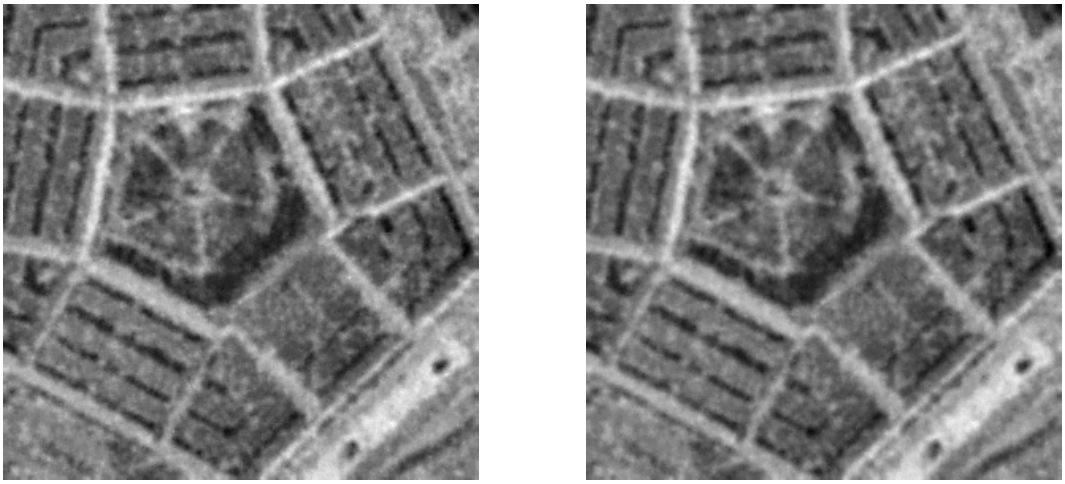

(a) **(b)**

Figure 13: (a) Proposed approach after 74 iterations. (b) Proposed approach after 100 iterations.

	ENL	MSE	β	SNR(db)
Noisy photo1	26.14	733.95	0.2754	14.11
Gamma filtered	48.28	354.37	0.3608	17.27
Modified-Lee filtered	50.06	305.51	0.4384	17.92
Enhanced-Frost filtered	48.50	306.67	0.3995	17.90
Proposed approach after 40^{th} iterations	51.26	302.67	0.4264	17.96
Proposed approach after 50^{th} iterations	52.59	299.11	0.4399	18.01
Proposed approach after 60^{th} iterations	53.41	297.44	0.4496	18.03
Proposed approach after 74^{th} iterations	54.96	296.42	0.4588	18.05
Proposed approach after 100^{th} iterations	56.29	298.41	0.4663	18.22

Table I: Some results of speckle reduction using photo1.

(a) **(b)**

Figure 14: (a) Original photo2. (b) Speckled version of photo2 with SNR=14.34 db.

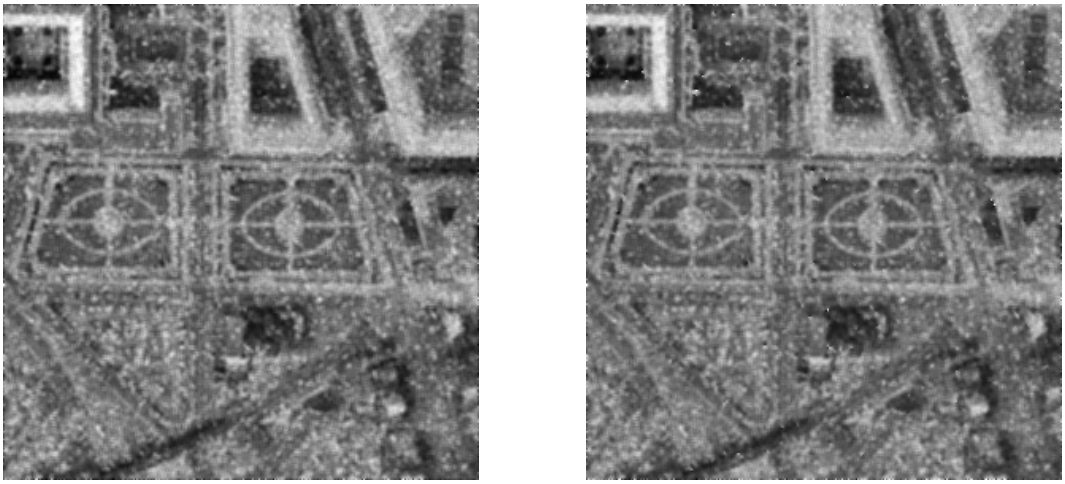

(a) **(b)**

Figure 15: ((a) Modified-Lee filtered version. (b) Gamma filtered version.

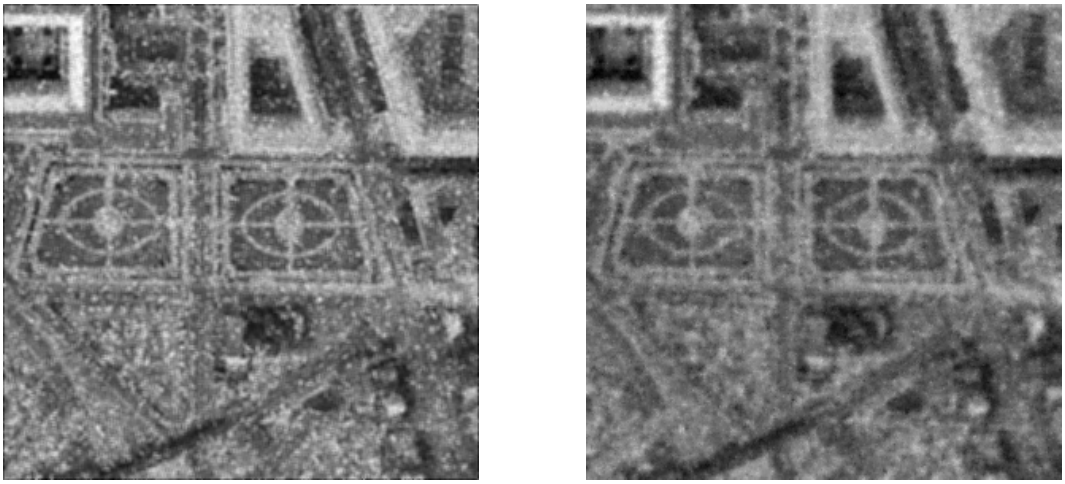

(a) **(b)**

Figure 16: (a) Enhanced Frost filtered version. (b) Proposed approach after 40 iterations.

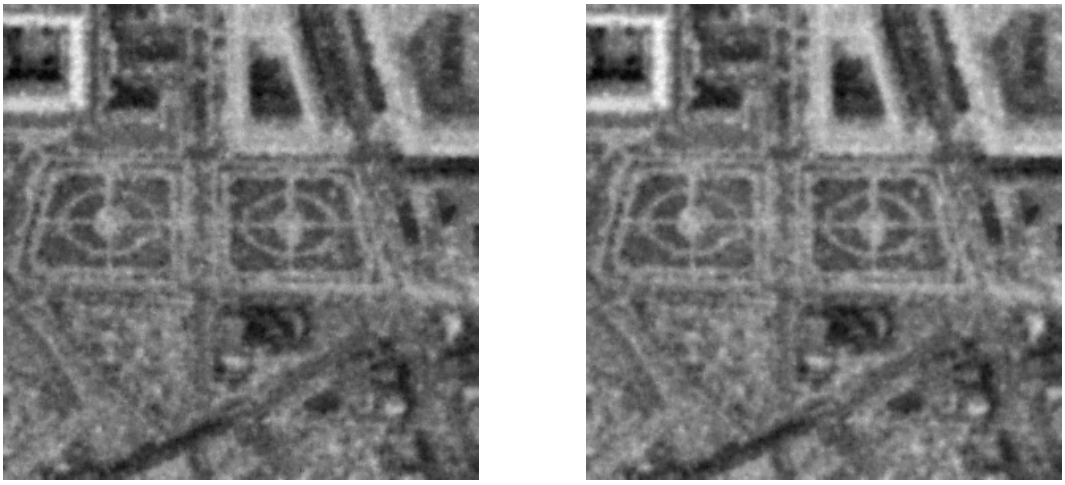

(a) **(b)**

Figure 17: (g) Proposed approach after 50 iterations. (h) Proposed approach after 60 iterations.

	ENL	MSE	β	SNR(db)
Noisy photo2	13.82	760.02	0.3139	14.34
Gamma filtered	24.48	309.66	0.4427	18.24
Modified-Lee filtered	25.13	308.32	0.4289	18.26
Enhanced-Frost filtered	24.92	313.41	0.3808	18.19
Proposed approach after 40^{th} iterations	84.79	297.64	0.4440	18.41
Proposed approach after 50^{th} iterations	91.45	294.78	0.4562	18.45
Proposed approach after 60^{th} iterations	97.15	294.46	0.4629	18.46

Table II: Some results of speckle reduction using photo2.

3.5 Application of speckle reduction to real SAR image

We have seen in Section 3.4 that our filtering approach behaves as expected on simulated speckled images. It will now be tested on a real SAR images [16, 6].

The results of the speckle reduction are shown in Figures 18-21 for the first real SAR image (SAR1). Table III gives a summary of the results obtained. It can be seen that after 21 iterations, the proposed approach yields a higher ENL than the other filters, which is an indication of a more efficient speckle reduction.

The second real SAR image (SAR2), is processed similarly. The results of the speckle reduction are shown in Figures 22-25 and Table IV gives a summary of the results. The ENL for the proposed approach after 19 iterations is, once again, larger than those obtained for the standard filters.

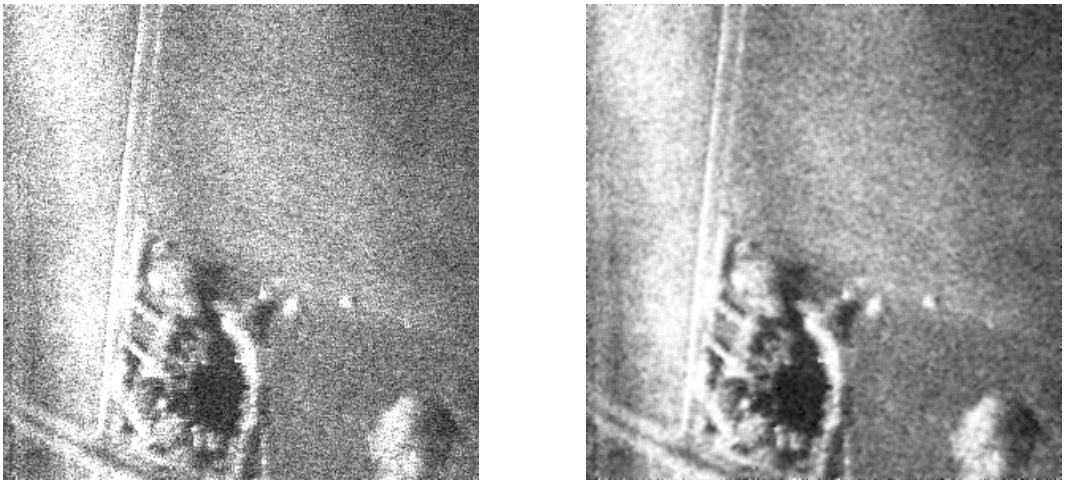

(a) **(b)**

Figure 18: (a) SAR1 (noisy). (b) Modified Lee filtered SAR1.

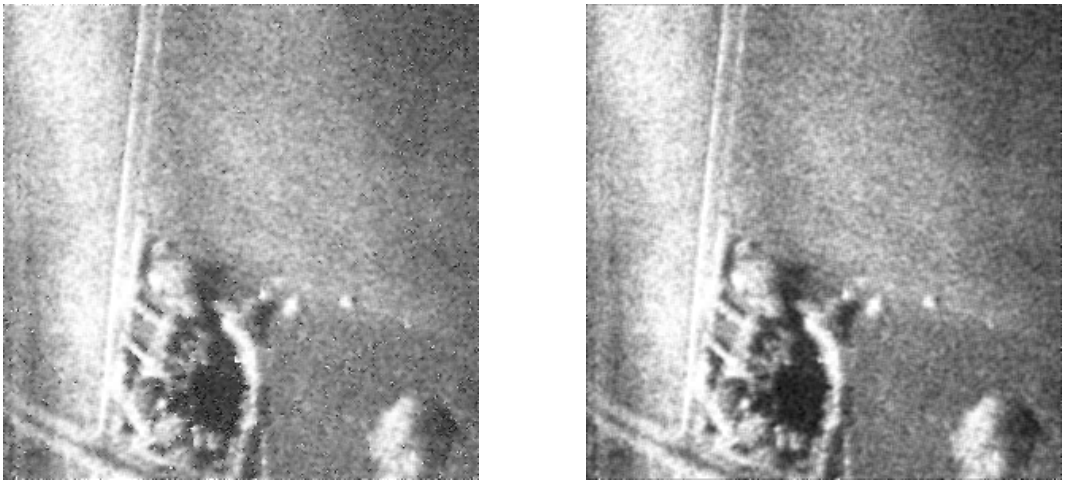

(a) **(b)**

Figure 19: (a) Gamma filtered SAR1. (b) Enhanced Frost filtered SAR1.

	ENL
SAR1	114.63
Gamma filtered SAR1	36.51
Modified Lee filtered SAR1	40.06
Enhanced Frost filtered SAR1	40.05
Proposed approach after 21^{st} iterations (SAR1)	40.29
Proposed approach after 31^{st} iterations (SAR1)	43.64
Proposed approach after 41^{st} iterations (SAR1)	45.55
Proposed approach after 51^{st} iterations (SAR1)	46.93

Table III: Some results of speckle reduction using SAR1.

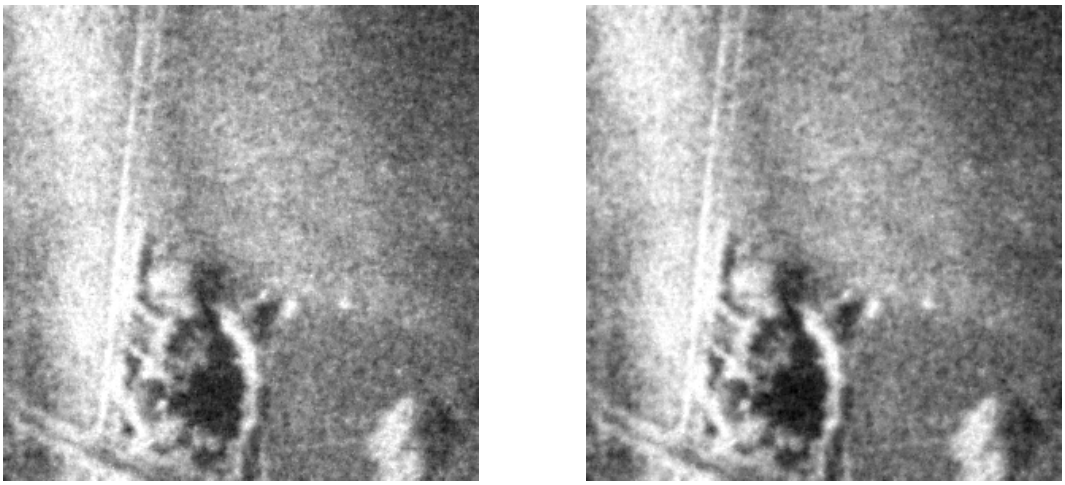

(a) **(b)**

Figure 20: (a) The proposed approach after 21 iterations. (b) The proposed approach after 31 iterations.

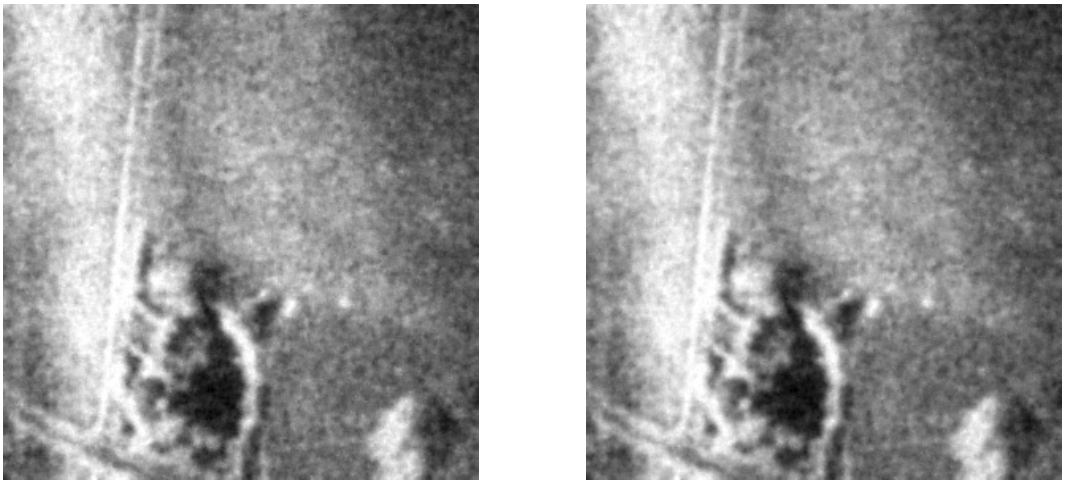

(a) **(b)**

Figure 21: (a) The proposed approach after 41 iterations. (b) The proposed approach after 51 iterations.

	ENL
SAR2	9.47
Gamma filtered SAR2	14.78
Modified Lee filtered SAR2	15.08
Enhance Frost filtered SAR2	13.96
Proposed approach after 19^{th} iterations (SAR2)	15.14
Proposed approach after 29^{th} iterations (SAR2)	15.79
Proposed approach after 39^{th} iterations (SAR2)	16.27
Proposed approach after 49^{th} iterations (SAR2)	16.57

Table IV: Some results of speckle reduction using SAR2.

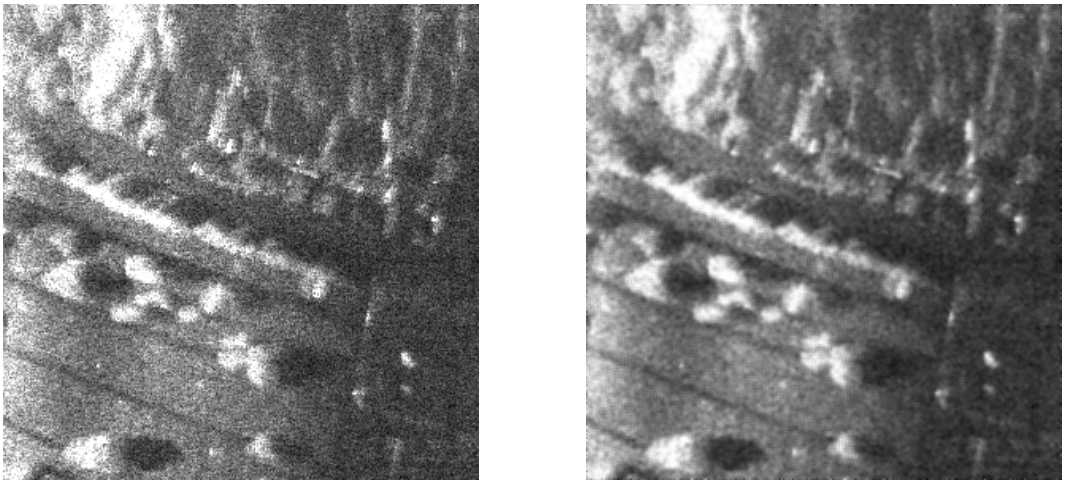

(a) **(b)**

Figure 22: (a) SAR2 (noisy). (b) Modified Lee filtered SAR2.

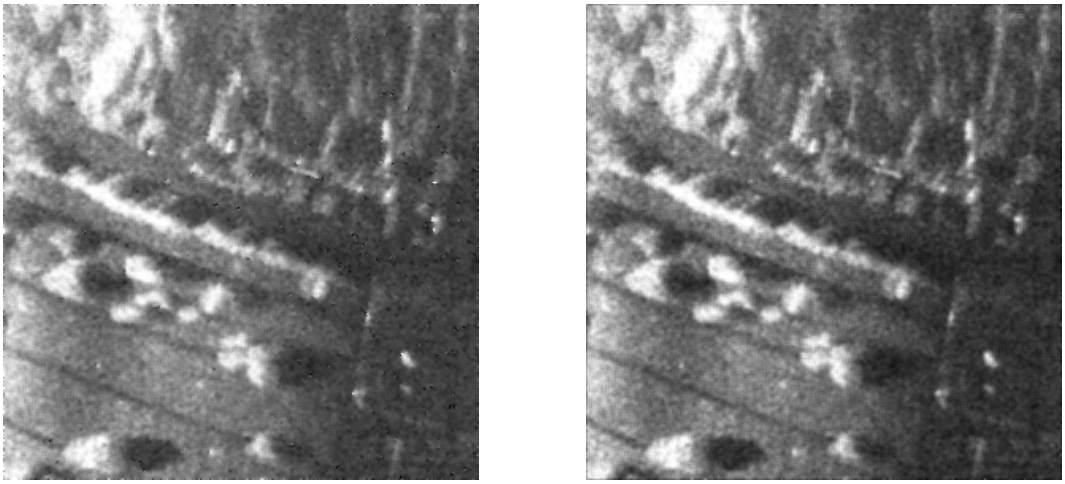

(a) **(b)**

Figure 23: (a) Gamma filtered image. (b) Enhanced Frost filtered SAR2.

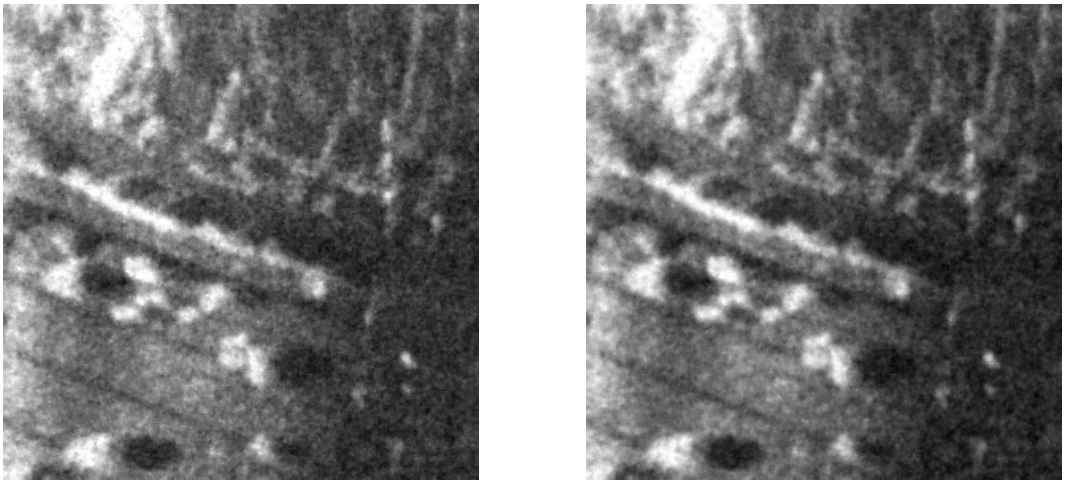

(a) **(b)**

Figure 24: (a) The proposed approach after 19 iterations. (b) The proposed approach after 29 iterations.

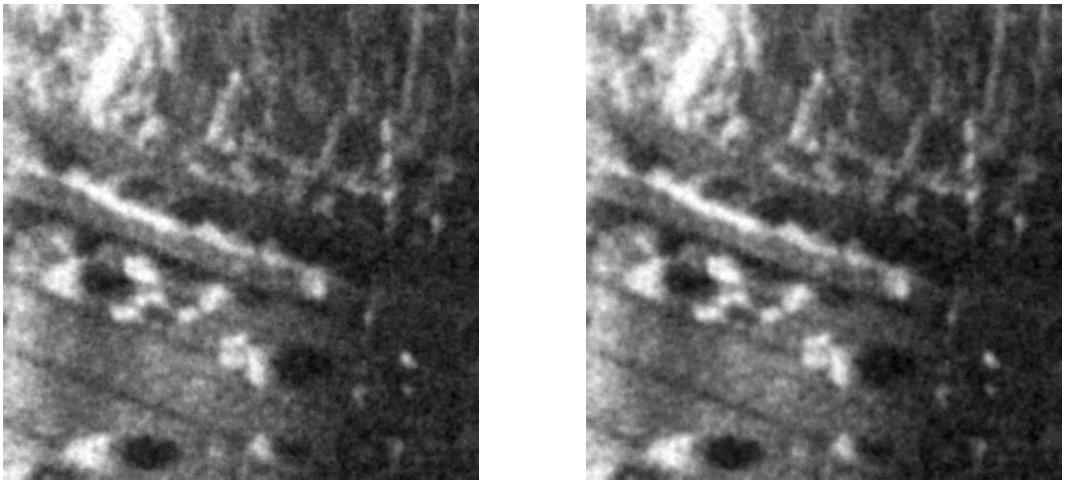

(a) **(b)**

Figure 25: (a) The proposed approach after 39 iterations. (b) The proposed approach after 49 iterations.

4 Conclusion

The contribution of this report is twofold. 1) It presents a novel model to model and simulate speckled images, in the context of Markov random field ; and 2) uses this model together with the Metropolis SA algorithm to reduce the speckle in simulated speckle imagery as well as in real SAR imagery. Various speckled images have been tested showing a similar trend. The reduction process using our proposed approach seems to outperform the Gamma Map, the modified Lee and the enhanced Frost filters. Three main reasons can explain this improved performance. Firstly, the intrinsic spatially-correlated and signal-dependent nature of speckle noise makes the MRF framework a natural choice. Secondly, the SA, being an iterative method, allows a gradual and interactive noise removal compared to the standard methods [8]. Thirdly, since the energy function used in the SA is derived according to the physical model of the speckle, which, in turn, leads to a reliable speckle reduction. The only bottleneck of the proposed approach is its computational complexity, which is currently under further investigation. An extension of this work to a dynamic model for speckle is also under investigation.

References

[1] http://vasc.ri.cmu.edu//idb/html/.

[2] Fabrizio Argenti and L. Alparone. Speckle removal from sar images in the undecimated wavelet domain. *IEEE Trans. Geosci. and Remote Sensing*, 40(11):2363–2374, Nov. 2002.

[3] J. Besag. Spatial interaction and the satatistical analysis of lattice systems. *J. R. Stat. Soc.*, pages 192–236, 1974.

[4] Thomas R. Crimmins. Geometric filter for reducing speckle. *Appl. Opt.*, 24(10):1438–1443, May 1985.

[5] J.C. Dainty. *Topic in Applied Physics: Laser Speckle and Related Phenomena*. Springer-Verlag, N.Y., 1984.

[6] D.G.Thompson *et al.* Yinsar: a compact low-cost interferometric synthetic aperture radar. *Proceedings of the International Geoscience and Remote Sensing Symposium*, pages 598–600, 1999.

[7] Alin Achim *et al.* Sar image denoising via bayesian wavelet shrinkage based on heavy tailed modeling. *IEEE Trans. Geosci. Remote Sensing*, 41:1773–1784, 2003.

[8] Chris Oliver *et al. Understanding Synthetic Aperture Radar Images*. SciTech, NC 27613, 2004.

[9] G. Franceschetti *et al. Synthetic Aperture Radar Processing*. CRC Press, New York, 1999.

[10] Kirkpatric *et al.* Optimation by simulated annealing. Research report rc, IBM, 1982.

[11] V.S. Frost, J.A. Stiles, K.S. Shanmugan, and J. C. Holtzman. A model for radar images and its application to adaptive digital filtering of multiplicative noise. *IEEE Trans. Pattern Anal. Machine Intell.*, 4:157–165, Mar. 1982.

[12] D. T. Kuan, A. A. Sawchuk, T. C. Strand, and P. Chavel. Adaptive noise smoothing filter for images with signal-dependent noise. *IEEE Trans. Pattern Anal. Machine Intell.*, PAMI-7:165–177, March 1985.

[13] Jong-Sen Lee. Speckle analysis and smoothing of synthetic aperture radar images, 1981. ©Academic Press, Inc.

[14] A. Lopes, E. Nezry, R. Touzi, and H. Laur. Structure detection and statistical adaptive speckle filtering in sar images. *International Journal of Remote Sensing*, 14(9):1735–1758, 1993.

[15] A. Lopes, R. Touzi, and E. Nezry. Adaptive Speckle Filters and Scene Heterogeneity. *IEEE Trans. Geosci. Remote Sensing*, 28:992–1000, Nov. 1990.

[16] Courtesy of David Long (Brigham Young U.). www.ee.byu.edu/ee/mers/yinsar/images/index.html, ©2002.

[17] Hua Xie, L.E. Pierce, and F.T. Ulaby. Sar speckle reduction using wavelet denoising and markov random field modeling. *IEEE Trans. on Geoscience an Remote Sensing*, 40(10):2196–2212, Oct. 2002.